

Supporting Information

Diamond-like Cuprous Coordination Polymer Based on [Cu₈I₆]²⁺ Cluster with Multistimuli-responsive Luminescence and Iodine Adsorption Behavior

Han-Wen Zheng, Dong-Dong Yang, Qiong-Fang Liang, Yan-Ping Liu,
Jia-Hui Shan, Qian-Qian Liu, Hong-Wei Tan, Ling Chen, and Xiang-Jun
Zheng*

Beijing Key Laboratory of Energy Conversion and Storage Materials, College of
Chemistry, Beijing Normal University, Beijing, 100875, China.

Corresponding author:

Tel.: +86-10-58805522; fax: +86-10-58802075.

E-mail address: xjzheng@bnu.edu.cn (X. -J. Zheng)

Contents

Fig. S1 The topological feature of complex **1**. Cyan spheres represent the [Cu₈I₆]²⁺ clusters, and blue lines represent the CN groups.

Fig. S2 Oscilloscope traces of SHG signals of KDP and **1**.

Fig. S3 (a) Differential scanning calorimetry (DSC) and (b) thermogravimetric analysis (TGA) of complex **1**.

Fig. S4 (a) PL and delayed (1 ms) excitation and emission spectra and (b) PL decay curve at 400 nm of ligand PPh₃ at 77 K.

Fig. S5 (a) PL and delayed (1 ms) excitation and emission spectra and (b) PL decay curve at 400 nm of **1** at 77 K.

Fig. S6 The intensity at 400 nm, 460 nm, 560 nm and 615 nm in the temperature range of 77-297 K.

Fig. S7 The halogen bonds in **1**.

Fig. S8 PL decay curves at room temperature (297 K) of (a) **1** at 560 nm and **1G** at 645 nm.

Fig. S9 Photographs of samples before and after adsorption and release process.

Fig. S10 The I₂ release UV-vis spectra of complex **1** (1 mg) in ethanol (3 mL), the insets of figures are dynamic intensity plots (monitored at 217 nm) over time.

Fig. S11 UV-vis spectra of iodine in ethanol at different concentrations.

Fig. S12 Calibration plot of standard iodine by UV-vis spectra.

Fig. S13 PXRD patterns of samples before and after adsorption and release process.

Fig. S14 Emission spectra of crystalline sample (**1**) before and after adsorption and release process ($\lambda_{\text{ex}} = 365$ nm).

Scheme S1 Calculated frontier orbitals for [Cu₈I₆(CN)₂(PPh₃)₄] unit.

Scheme S2 Possible luminescence energy transition diagram for complex **1**.

Table S1 Crystal data and structure refinement parameters of complex **1** and **1a**.

Table S2 Selected Bond Lengths (Å) and Angles (deg) of complex **1**.

Table S3 Selected Bond Lengths (Å) and Angles (deg) of complex **1a**.

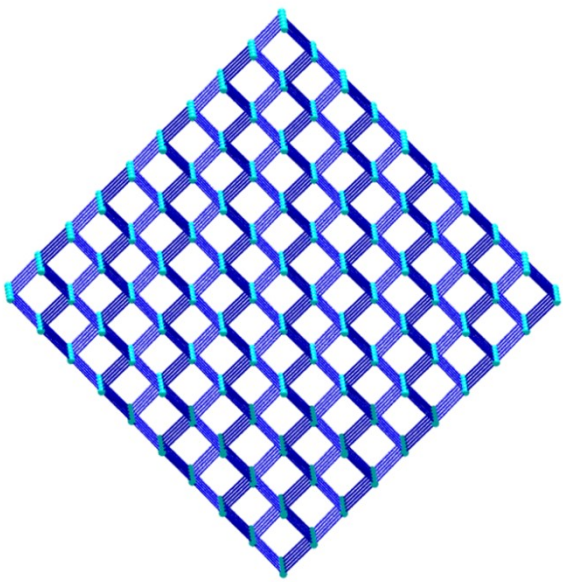


Fig. S1 The topological feature of complex **1**. Cyan spheres represent the $[\text{Cu}_8\text{I}_6]^{2+}$ clusters, and blue lines represent the CN groups.

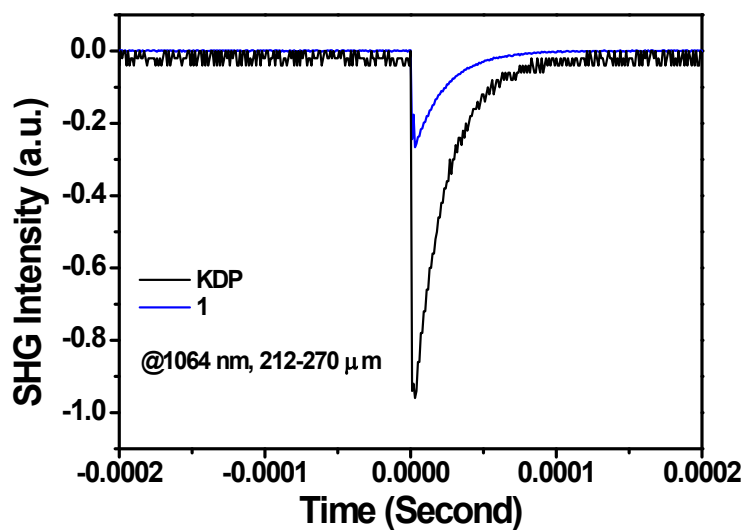


Fig. S2 Oscilloscope traces of SHG signals of KDP and **1**.

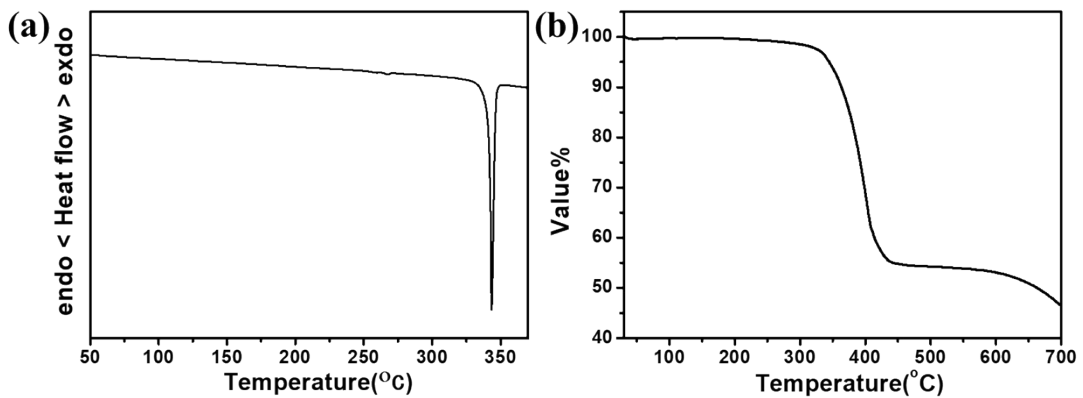


Fig. S3 (a) Differential scanning calorimetry (DSC) and (b) thermogravimetric analysis (TGA) of complex **1**.

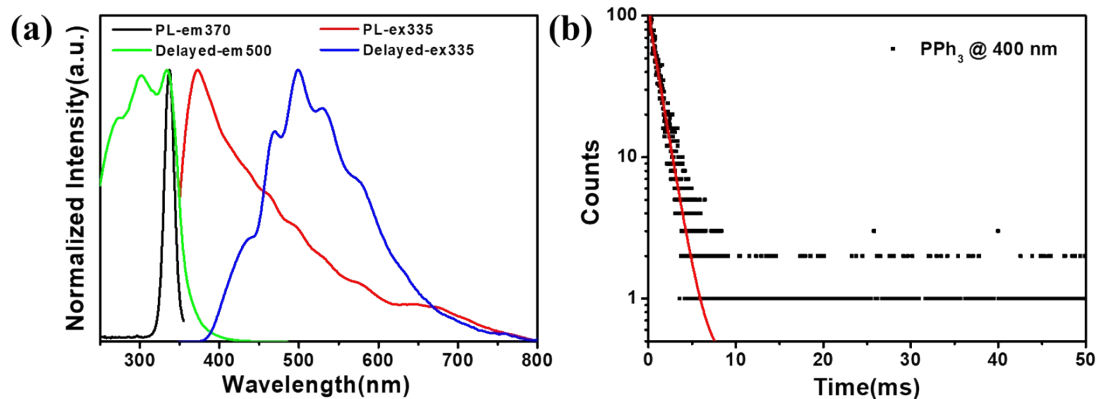


Fig. S4 (a) PL and delayed (1 ms) excitation and emission spectra and (b) PL decay curve at 400 nm of ligand PPh_3 at 77 K.

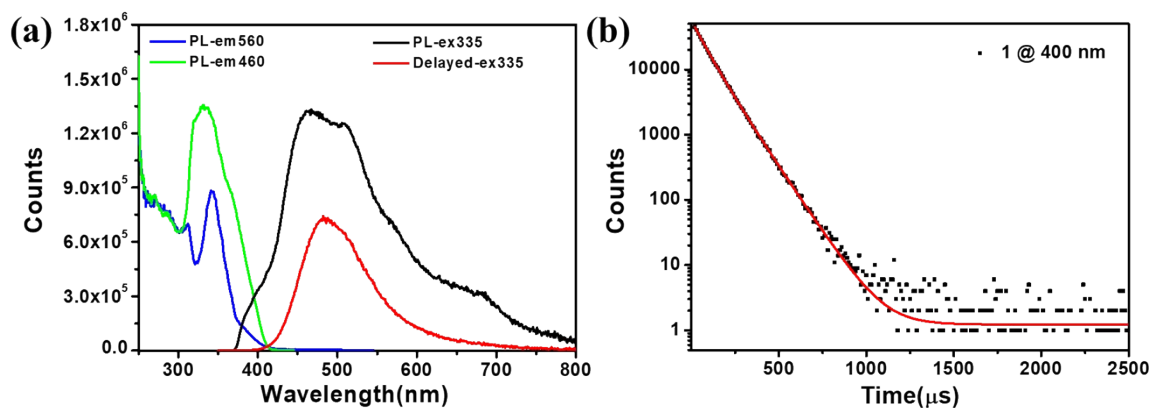


Fig. S5 (a) PL and delayed (1 ms) excitation and emission spectra and (b) PL decay curve at 400 nm of **1** at 77 K.

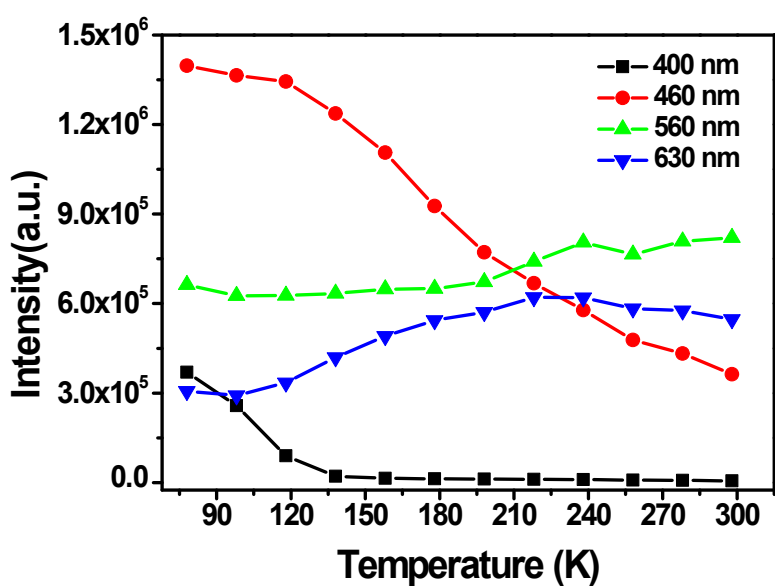


Fig. S6 The intensity at 400 nm, 460 nm, 560 nm and 615 nm in the temperature range of 77-297 K.

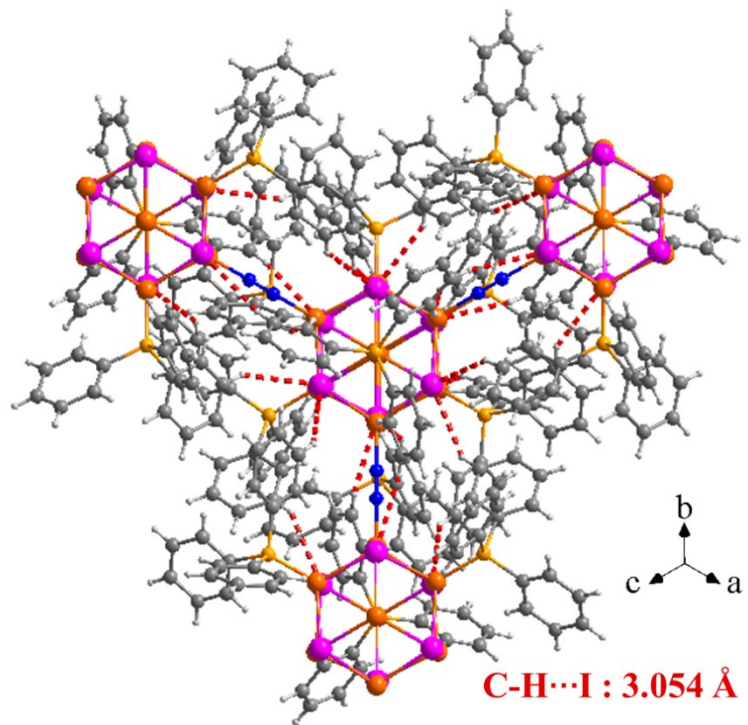


Fig. S7 The halogen bonds in **1**.

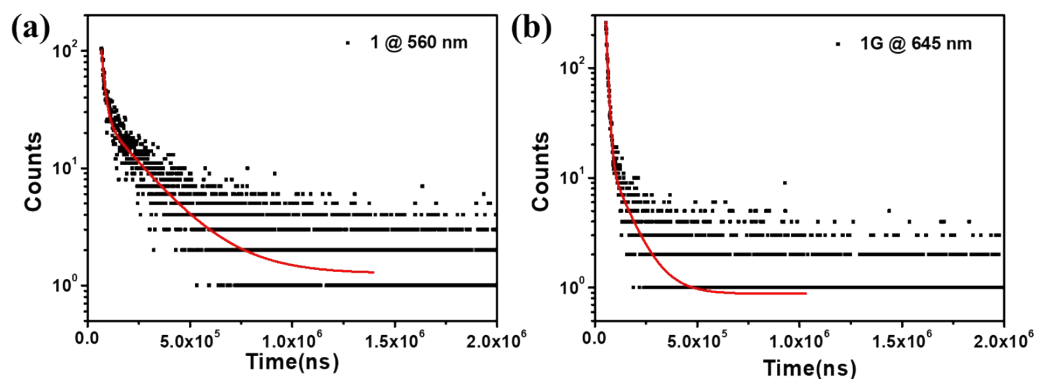


Fig. S8 PL decay curves at room temperature (297 K) of (a) **1** at 560 nm and **1G** at 645 nm.

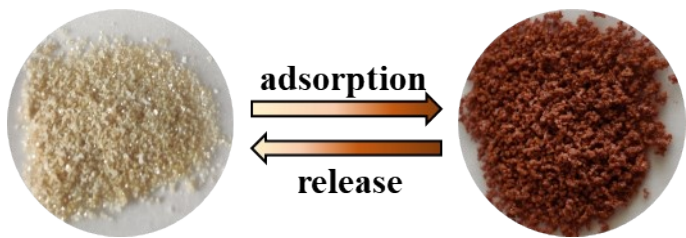


Fig. S9 Photographs of samples before and after adsorption and release process.

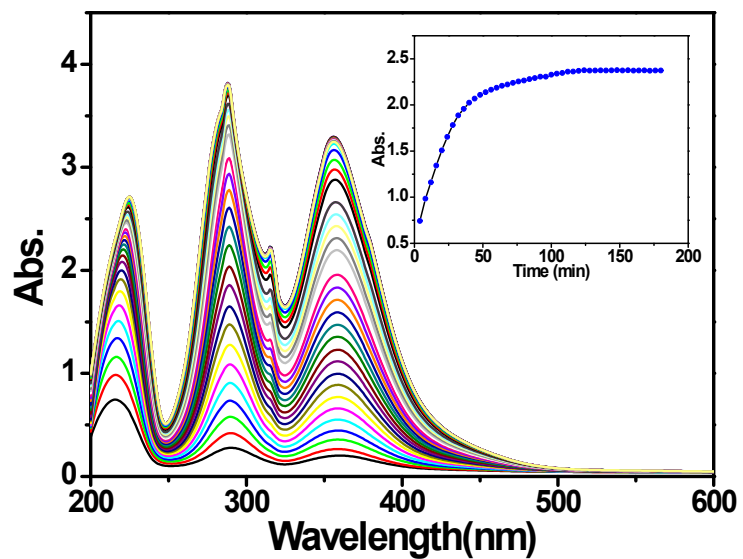


Fig. S10 The I_2 release UV-vis spectra of complex **1** (1 mg) in ethanol (3 mL), the insets of figures are dynamic intensity plots (monitored at 217 nm) over time.

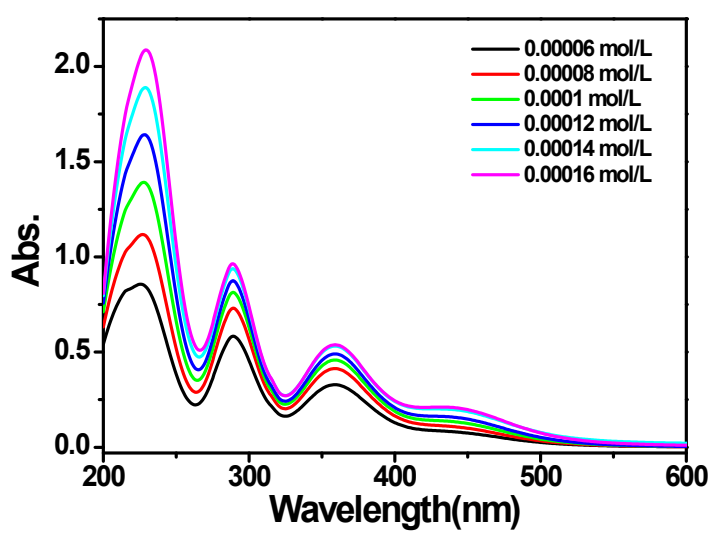


Fig. S11 UV-vis spectra of iodine in ethanol at different concentrations.

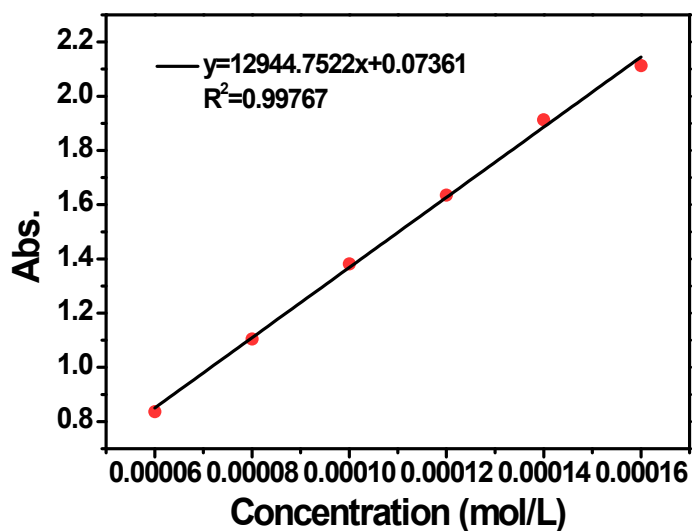


Fig. S12 Calibration plot of standard iodine by UV-vis spectra.

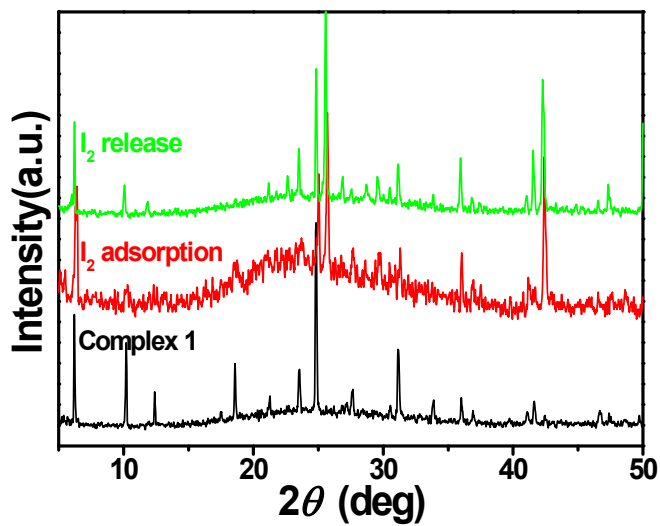


Fig. S13 PXRD patterns of samples before and after adsorption and release process.

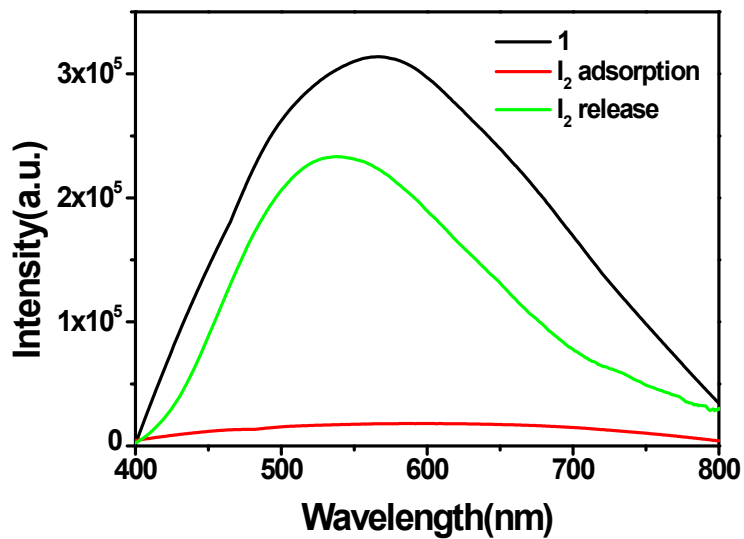
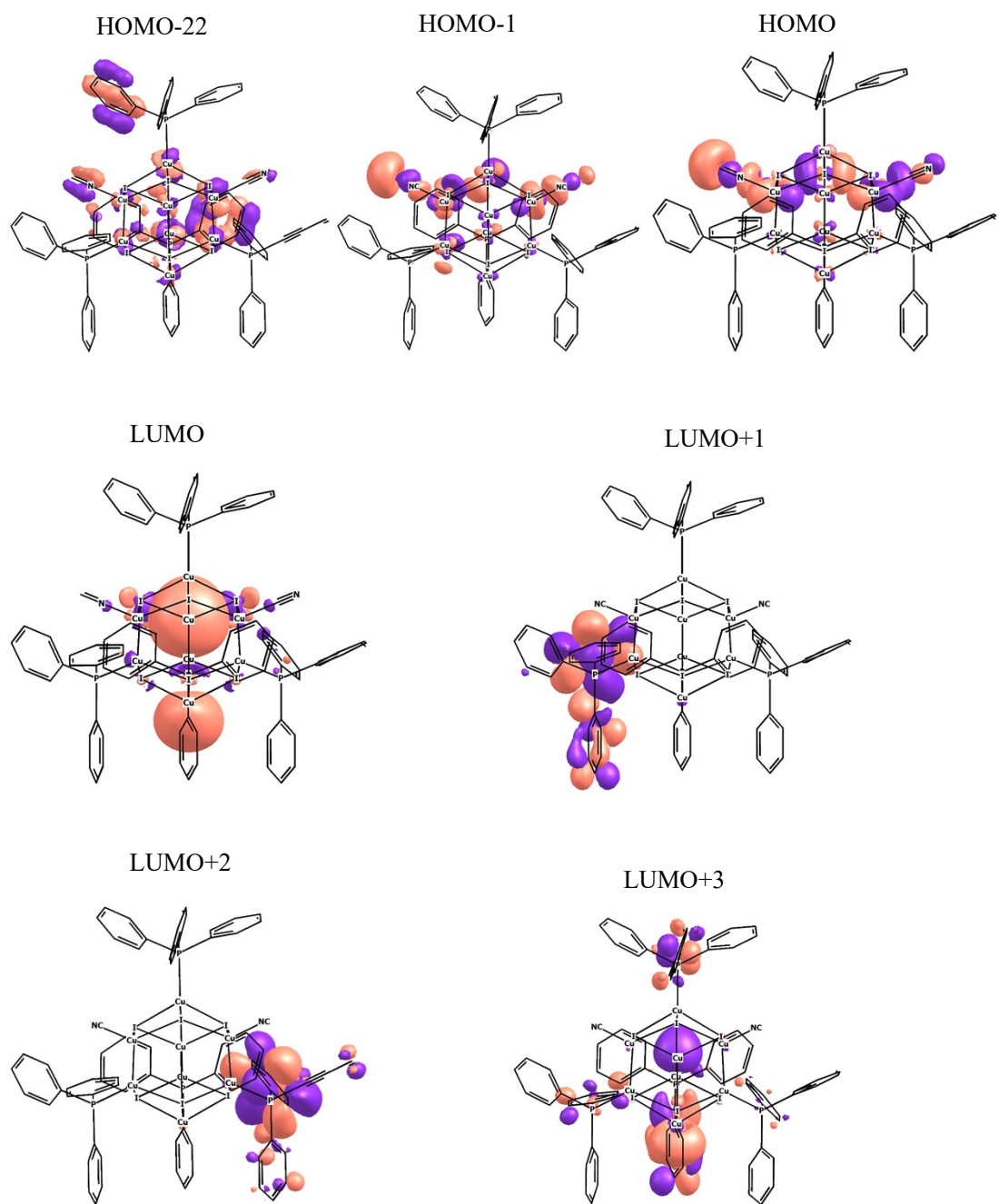
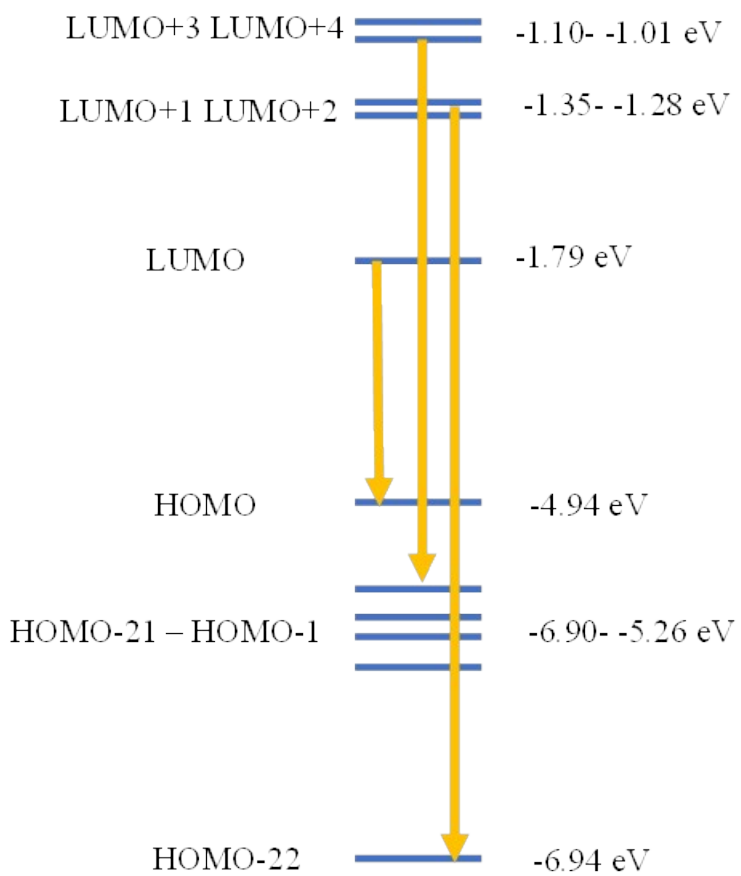


Fig. S14 Emission spectra of crystalline sample (**1**) before and after adsorption and release process ($\lambda_{\text{ex}} = 365 \text{ nm}$).



Scheme S1 Calculated frontier orbitals for $[\text{Cu}_8\text{I}_6(\text{CN})_2(\text{PPh}_3)_4]$ unit.



Scheme S2 Possible luminescence energy transition diagram for complex 1.

Table S1 Crystal data and structure refinement parameters of complex **1** and **1a**.

Compound	1	1a
Empirical formula	C ₇₄ H ₆₀ Cu ₈ I ₆ N ₂ P ₄	C ₇₄ H ₆₀ Cu ₈ I ₆ N ₂ P ₄
Formula weight	2370.84	2370.71
Temperature/K	100.00(10)	272.5(5)
Crystal system	Cubic	Cubic
Space group	<i>Fd</i> $\bar{3}$	<i>Fd</i> $\bar{3}m$
a/ \AA	24.6471(5)	24.91275(9)
b/ \AA	24.6471(5)	24.91275(9)
c/ \AA	24.6471(5)	24.91275(9)
$\alpha/^\circ$	90	90
$\beta/^\circ$	90	90
$\gamma/^\circ$	90	90
Volume/ \AA^3	14972.6(9)	15461.98(17)
Z	8	8
ρ_{calc} g/cm ³	2.104	2.037
μ/mm^{-1}	23.003	22.275
F(000)	9024.0	9024.0
Radiation	CuK α ($\lambda = 1.54184$)	CuK α ($\lambda = 1.54184$)
2 θ range for data collection/ $^\circ$	10.152 to 132.904	11.782 to 152.906
Index ranges	-28 $\leq h \leq 23$, -18 $\leq k \leq 11$, -29 $\leq l \leq 13$	-31 $\leq h \leq 31$, -31 $\leq k \leq 31$, -30 $\leq l \leq 30$
Reflections collected	3841	44589
Independent reflections	1077 [R _{int} = 0.0561, R _{sigma} = 0.0288]	821 [R _{int} = 0.1138, R _{sigma} = 0.0145]
Data/restraints/parameters	1077/0/72	821/0/71
Goodness-of-fit on F ²	1.119	1.123
Final R indexes [I >= 2 σ (I)]	R ₁ = 0.0370, wR ₂ = 0.0958	R ₁ = 0.0417, wR ₂ = 0.1069
R indices (all data)	R ₁ = 0.0377, wR ₂ = 0.0964	R ₁ = 0.0437, wR ₂ = 0.1080
Largest diff. peak/hole (e \AA^{-3})	0.89/-1.48	0.87/-1.20
CCDC number	2127744	2132839

Table S2 Selected Bond Lengths (\AA) and Angles (deg) of complex **1**.

I1—Cu1 ⁱ	2.6731 (5)	Cu1—I1 ⁱⁱⁱ	2.6731 (5)
I1—Cu1	2.6731 (5)	Cu1—P1	2.241 (2)

I1—Cu2	2.6894 (6)	Cu2—I1 ⁱⁱ	2.6894 (6)
I1—Cu2 ⁱ	2.6894 (6)	Cu2—I1 ^{iv}	2.6894 (6)
Cu1—I1 ⁱⁱ	2.6731 (5)	Cu2—N7	1.943 (9)
Cu1 ⁱ —I1—Cu1	117.02 (4)	C2 ^v —P1—Cu1	114.40 (13)
Cu1 ⁱ —I1—Cu2	74.535 (19)	C2 ⁱⁱⁱ —P1—Cu1	114.40 (13)
Cu1—I1—Cu2 ⁱ	74.536 (19)	C2—P1—Cu1	114.40 (13)
Cu1—I1—Cu2	74.535 (19)	I1 ^{iv} —Cu2—I1 ⁱⁱ	104.54 (3)
Cu1 ⁱ —I1—Cu2 ⁱ	74.536 (19)	I1 ^{iv} —Cu2—I1	104.54 (3)
Cu2—I1—Cu2 ⁱ	118.61 (6)	I1 ⁱⁱ —Cu2—I1	104.54 (3)
I1 ⁱⁱ —Cu1—I1	105.45 (3)	N7—Cu2—I1	114.04 (3)
I1 ⁱⁱⁱ —Cu1—I1	105.45 (3)	N7—Cu2—I1 ^{iv}	114.04 (3)
I1 ⁱⁱⁱ —Cu1—I1 ⁱⁱ	105.45 (3)	N7—Cu2—I1 ⁱⁱ	114.04 (3)
P1—Cu1—I1 ⁱⁱ	113.25 (2)	N7 ^{vi} —N7—Cu2	180.0 (16)
P1—Cu1—I1	113.25 (2)	C7 ^{vi} —N7—Cu2	180.0 (16)
P1—Cu1—I1 ⁱⁱⁱ	113.25 (2)		

Symmetry codes: (i) $x, -y+1/4, -z+1/4$; (ii) $y+1/2, z, x-1/2$; (iii) $z+1/2, -x+3/4, -y+1/4$; (iv) $z+1/2, x-1/2, y$; (v) $-y+3/4, -z+1/4, x-1/2$; (vi) $-x+1, -y, -z$.

Table S3 Selected Bond Lengths (\AA) and Angles (deg) of complex **1a**.

I1—Cu1 ⁱ	2.6880 (9)	Cu1—I1 ⁱⁱⁱ	2.6880 (9)
I1—Cu1	2.6880 (9)	Cu1—P1	2.248 (4)
I1—Cu2 ⁱⁱ	2.7233 (12)	Cu2—I1 ⁱⁱⁱ	2.7232 (12)
I1—Cu2	2.7232 (12)	Cu2—I1 ⁱ	2.7232 (12)
Cu1—I1 ⁱⁱ	2.6880 (9)	Cu2—N7	2.085 (15)
Cu1—I1—Cu1 ⁱ	117.33 (8)	I1 ⁱ —Cu2—I1	103.35 (6)
Cu1 ⁱ —I1—Cu2	75.08 (3)	I1 ⁱⁱⁱ —Cu2—I1	103.35 (6)
Cu1—I1—Cu2	75.08 (3)	I1 ⁱⁱⁱ —Cu2—I1 ⁱ	103.35 (6)
Cu1 ⁱ —I1—Cu2 ⁱⁱ	75.08 (3)	N7—Cu2—I1 ⁱ	115.06 (5)
Cu1—I1—Cu2 ⁱⁱ	75.08 (3)	N7—Cu2—I1	115.06 (5)
Cu2—I1—Cu2 ⁱⁱ	120.65 (11)	N7—Cu2—I1 ⁱⁱⁱ	115.06 (5)
I1 ⁱⁱⁱ —Cu1—I1	105.27 (5)	C7—Cu2—I1 ⁱ	115.06 (5)
I1 ⁱⁱ —Cu1—I1	105.27 (5)	C7—Cu2—I1	115.06 (5)
I1 ⁱⁱ —Cu1—I1 ⁱⁱⁱ	105.27 (5)	C7—Cu2—I1 ⁱⁱⁱ	115.06 (5)
P1—Cu1—I1 ⁱⁱ	113.40 (4)	C2—P1—Cu1	114.2 (3)
P1—Cu1—I1	113.40 (4)	C2 ^{vii} —P1—Cu1	114.2 (3)
P1—Cu1—I1 ⁱⁱⁱ	113.40 (4)	C2 ^{iv} —P1—Cu1	114.2 (3)
C2 ^{vi} —P1—Cu1	114.2 (3)	C2 ^{viii} —P1—Cu1	114.2 (3)
C2 ^v —P1—Cu1	114.2 (3)		

Symmetry codes: (i) $-y+3/4, x-1/2, -z+1/4$; (ii) $y+1/2, -x+3/4, -z+1/4$; (iii) $-z+3/4, -y+1/4, x-1/2$; (iv) $z+1/2, y, x-1/2$; (v) $x, -z+1/4, -y+1/4$; (vi) $z+1/2, -x+3/4, -y+1/4$; (vii) $-y+3/4, -x+3/4, z$; (viii) $-y+3/4, -z+1/4, x-1/2$.